Actin Cytoskeleton-Dependent Dynamics of the Human Serotonin$_{1A}$ Receptor Correlates with Receptor Signaling

Sourav Ganguly, Thomas J. Pucadyil, and Amitabha Chattopadhyay
Centre for Cellular and Molecular Biology, Hyderabad 500 007, India

ABSTRACT Analyzing the dynamics of membrane proteins in the context of cellular signaling represents a challenging problem in contemporary cell biology. Lateral diffusion of lipids and proteins in the cell membrane is known to be influenced by the cytoskeleton. In this work, we explored the role of the actin cytoskeleton on the mobility of the serotonin$_{1A}$ (5-HT$_{1A}$) receptor, stably expressed in CHO cells, and its implications in signaling. FRAP analysis of 5-HT$_{1A}$R-EYFP shows that destabilization of the actin cytoskeleton induced by either CD or elevation of cAMP levels mediated by forskolin results in an increase in the mobile fraction of the receptor. The increase in the mobile fraction is accompanied by a corresponding increase in the signaling efficiency of the receptor. Interestingly, with increasing concentrations of CD used, the increase in the mobile fraction exhibited a correlation of ~0.95 with the efficiency in ligand-mediated signaling of the receptor. Radioligand binding and G-protein coupling of the receptor were found to be unaffected upon treatment with CD. Our results suggest that signaling by the serotonin$_{1A}$ receptor is correlated with receptor mobility, implying thereby that the actin cytoskeleton could play a regulatory role in receptor signaling. These results may have potential significance in the context of signaling by GPCRs in general and in the understanding of GPCR-cytoskeleton interactions with respect to receptor signaling in particular.

INTRODUCTION

Biological membranes are complex two-dimensional noncovalent assemblies of a diverse variety of lipids and proteins. Current understanding of the organization of biological membranes involves the concept of lateral heterogeneities in the membrane, collectively termed ''membrane domains''. These specialized regions are believed to be enriched in specific lipids and proteins and facilitate processes such as trafficking, sorting, and signal transduction over a range of spatiotemporal scale (1–4). The eukaryotic plasma membrane, therefore, displays a rather complex architecture in terms of the organization of membrane components.

Seven transmembrane domain GPCRs constitute one of the largest families of proteins in mammals and account for ~2% of the total proteins coded by the human genome (5). Signal transduction events mediated by GPCRs are the primary means by which cells communicate with and respond to their external environment (6). As a consequence, GPCRs represent major targets for the development of novel drug candidates in all clinical areas (7). The major paradigm in GPCR signaling is that their stimulation leads to the recruitment and activation of heterotrimeric G-proteins (8). The key steps involved in this process are agonist-induced guanine nucleotide exchange of GDP by GTP on the G-protein α subunit. This is followed by conformational changes in the GPCR and dissociation or rearrangement of the G_{α} from $G_{\beta\gamma}$ subunits. The activated G-protein subunits subsequently elicit separate downstream signaling events by interacting with specific effectors like AC, phospholipases, or ion channels.

The G-protein-coupled serotonin$_{1A}$ (5-HT$_{1A}$) receptor is the most extensively studied among the serotonin receptors (9). Serotonin$_{1A}$ receptors appear to play a key role in the generation and modulation of various cognitive, behavioral, and developmental functions, such as sleep, mood, addiction, depression, and anxiety (10). Mutant (knockout) mice lacking the serotonin$_{1A}$ receptor exhibit enhanced anxiety-related behavior and provide an important animal model for the analysis of complex traits such as anxiety disorders and aggression in higher organisms (11). Interestingly, serotonin$_{1A}$ receptor-mediated signaling has been implicated in various neurodevelopmental processes such as neurite growth and neuronal survival (12). Upon binding serotonin, the serotonin$_{1A}$ receptor signals via $G_{\alpha i}$-mediated inhibition of AC, leading to the lowering of cAMP levels and consequent downstream signaling (9). We have previously characterized the heterolo-

Submitted November 13, 2007, and accepted for publication February 21, 2008.

Address reprint requests to Amitabha Chattopadhyay, Centre for Cellular and Molecular Biology, Uppal Road, Hyderabad 500 007, India. Tel.: +91-40-2719-2578; Fax: +91-40-2716-0311; E-mail: amit@ccmb.res.in.

Thomas J. Pucadyil's present address is Department of Cell Biology, The Scripps Research Institute, La Jolla, CA 92037.

Abbreviations used: CHO, Chinese hamster ovary; EYFP, enhanced yellow fluorescent protein; G-protein, guanine nucleotide binding protein; IC_{50}, 50% inhibitory concentration; RhoA, ras homolog gene family, member A; ROI, region of interest; 5-HT, 5-hydroxytryptamine; 5-HT$_{1A}$R-EYFP, 5-hydroxytryptamine$_{1A}$ receptor tagged to enhanced yellow fluorescent protein; 8-OH-DPAT, 8-hydroxy-2-(di-*N*-propylamino)tetralin; AC, adenylyl cyclase; BCA, bicinchoninic acid; cAMP, adenosine 3′,5′-cyclic monophosphate; CD, cytochalasin D; D_{app}, apparent diffusion coefficient; DMSO, dimethyl sulphoxide; GPCR, G-protein coupled receptor; GTP-γ-S, guanosine 5′-*O*-(3-thiotriphosphate); FRAP, fluorescence recovery after photobleaching; IBMX, 3-isobutyl-1-methylxanthine; *p*-MPPI, 4-(2′-methoxy)-phenyl-1-[2′-(*N*-2″-pyridinyl)-*p*-iodobenzamido]ethyl-piperazine; *p*-MPPF, 4-(2′-methoxy)-phenyl-1-[2′-(*N*-2″-pyridinyl)-*p*-fluorobenzamido]ethyl-piperazine; PBS, phosphate-buffered saline; PDZ, PSD95/DlgA/ZO-1; PKA, protein kinase A; PMSF, phenylmethanesulfonyl fluoride.

Editor: G. Barisas.

0006-3495/08/07/451/13 $2.00

doi: 10.1529/biophysj.107.125732

gously expressed serotonin$_{1A}$ receptor tagged to EYFP in CHO cells pharmacologically and shown that the tagged receptors are essentially similar to the native receptor in hippocampal membranes (13).

The plasma membrane is the first platform where a cell initiates its reaction to an extracellular stimulus. Since membrane-bound molecules are dynamic, functional association between them depends on the probability of their interaction with signaling partners. Cellular signaling mediated by proteins has therefore been hypothesized to be a consequence of differential mobility parameters of the various interacting components (14–16). This forms the basis of the ''mobile receptor'' hypothesis, which proposes that receptor-effector interactions at the plasma membrane are controlled by lateral mobility of the interacting components. Lateral diffusion of membrane lipids and proteins is known to be influenced by cytoskeletal proteins. Early results from studies performed on myoblast and erythrocyte membranes have suggested that the cytoskeleton imposes constraints on the lateral dynamics of membrane proteins (17,18). Recent observations using sophisticated microscopic techniques have further supported the notion of an actin cytoskeleton-dependent dynamics of molecules in cell membranes (19) and have led to the ''anchored protein picket fence model'' of membranes (20). An interesting corollary of this model is that even proteins which do not interact specifically with the actin cytoskeleton are expected to exhibit actin cytoskeleton-dependent dynamics. The destabilization of the actin cytoskeleton may thus provide a handle to manipulate the lateral dynamics of membrane proteins. In this work, we used this strategy to address the mechanism of signaling of the serotonin$_{1A}$ receptor expressed in CHO cells. We report here the effect of actin cytoskeleton destabilization on the diffusion properties of the functional serotonin$_{1A}$ receptor analyzed by FRAP. In addition, we monitored the ability of the receptor to signal under conditions of actin destabilization by estimating its ability to lower cAMP levels upon activation by serotonin in live cells. We interpret our results based on the current understanding of actin-dependent lateral dynamics of membrane proteins and receptor-effector interactions.

MATERIALS AND METHODS

Materials

$MgCl_2$, *p*-MPPI, $CaCl_2$, penicillin, streptomycin, gentamycin sulfate, serotonin, polyethylenimine, and CD were obtained from Sigma (St. Louis, MO). Rhodamine-conjugated phalloidin was from Molecular Probes (Eugene, OR). D-MEM/F-12 (Dulbecco's modified Eagle medium: nutrient mixture F-12 (Ham) (1:1)), fetal calf serum, and geneticin (G 418) were from Invitrogen Life Technologies (Carlsbad, CA). GTP-γ-S was from Roche Applied Science (Mannheim, Germany). BCA reagent was from Pierce (Rockford, IL). Forskolin and IBMX were obtained from Calbiochem (San Diego, CA). [^{3}H]8-OH-DPAT (specific activity = 135.0 Ci/mmol) and [^{3}H]*p*-MPPF (specific activity = 70.5 Ci/mmol) were purchased from DuPont New England Nuclear (Boston, MA). The cyclic [^{3}H]AMP assay kit was purchased from Amersham Biosciences (Buckinghamshire, UK). GF/B glass microfiber filters were from Whatman International (Kent, UK). All other chemicals used were of the highest available purity. Water was purified through a Millipore (Bedford, MA) Milli-Q system and used throughout.

Cells and cell culture

CHO-K1 cells stably expressing the 5-HT$_{1A}$R-EYFP (referred to as CHO-5-HT$_{1A}$R-EYFP) were used ($\sim 10^5$ receptors/cell). Cells were grown in D-MEM/F-12 (1:1) supplemented with 2.4 g/l of sodium bicarbonate, 10% fetal calf serum, 60 μg/ml penicillin, 50 μg/ml streptomycin, 50 μg/ml gentamycin sulfate in a humidified atmosphere with 5% CO_2 at 37°C. CHO-5-HT$_{1A}$R-EYFP cells were maintained in the above-mentioned conditions with 300 μg/ml geneticin.

CD treatment of cells

A stock solution of 2 mM CD was made in DMSO, and further concentrations were prepared upon dilution of the stock in buffer A (PBS containing 1 mM $CaCl_2$ and 0.5 mM $MgCl_2$). The amount of DMSO was always $<0.5\%$ (v/v). Treatment of control cells with similar amounts of DMSO did not show any change in cellular morphology or receptor dynamics.

Cell membrane preparation

Cell membranes were prepared as described earlier (13) with a few modifications. Cells grown to confluence in 175 cm^2 flasks were harvested with ice cold buffer B (10 mM Tris, 5 mM EDTA, 0.1 mM PMSF, pH 7.4) at room temperature. The harvest was homogenized with a Polytron (Duluth, GA) homogenizer for 20 s at 4°C at maximum speed. The cell lysate was then centrifuged at 500 *g* for 10 min at 4°C, and the resulting supernatant was centrifuged at 40,000 *g* for 30 min at 4°C. The pellet thus obtained was suspended in 50 mM Tris, pH 7.4, buffer and used for radioligand binding assays. The total protein concentration of cell membranes was determined using BCA assay (21).

Radioligand binding assay

Receptor binding assays were carried out as described earlier (13) with some modifications. Briefly, tubes in duplicate with 40 μg of total protein in a volume of 1 ml buffer C (50 mM Tris, 1 mM EDTA, 10 mM $MgCl_2$, 5 mM $MnCl_2$, pH 7.4) for agonist binding or in 1 ml buffer D (50 mM Tris, 1 mM EDTA, pH 7.4) for antagonist binding assays were used. Tubes were incubated with the radiolabeled agonist [^{3}H]8-OH-DPAT (final concentration in the assay tube was 0.29 nM) or antagonist [^{3}H]*p*-MPPF (final concentration in the assay tube was 0.5 nM) for 1 h at 25°C. Nonspecific binding was determined by performing the assay either in the presence of 10 μM serotonin (for agonist binding) or in the presence of 10 μM *p*-MPPI (for antagonist binding). The binding reaction was terminated by rapid filtration under vacuum in a Brandel cell harvester (Gaithersburg, MD) through Whatman GF/B 2.5 cm diameter glass microfiber filters (1.0 μm pore size), which were presoaked in 0.15% (w/v) polyethylenimine for 1 h. The filters were then washed three times with 3 ml of cold water (4°C) and dried, and the retained radioactivity was measured in a Packard (Meriden, CT) Tri-Carb 1500 liquid scintillation counter using 5 ml of scintillation fluid.

GTP-γ-S sensitivity assay

For experiments in which GTP-γ-S was used, agonist binding assays were performed on membranes prepared from cells treated with CD, in the presence of varying concentrations of GTP-γ-S in buffer C containing 0.29 nM [^{3}H]8-OH-DPAT. Membranes prepared from cells without CD treatment served as control. The concentration of GTP-γ-S leading to 50% inhibition of specific agonist binding (IC_{50}) was calculated by nonlinear regression fitting of the data to a four-parameter logistic function as described earlier (13):

$$B = a/(1 + (x/I)^s) + b, \quad (1a)$$

where B is specific binding of the agonist normalized to binding in the presence of very low concentration (10^{-12} M) of GTP-γ-S, x denotes the concentration of GTP-γ-S, a is the range (y_{max}–y_{min}) of the fitted curve on the ordinate (y axis), I is the IC_{50} concentration, b is the background of the fitted curve (y_{min}), and s is the slope factor.

Estimation of cAMP levels in cells

The ability of the agonist to downregulate the forskolin-stimulated increase in cAMP levels in cells was assessed as described previously (13), with a few modifications. CHO cells stably expressing 5-HT$_{1A}$R-EYFP were plated at a density of 10^5 cells in 24-well plates and grown in D-MEM/F-12 medium for 48 h. After treatment with specified concentrations of CD for 30 min in buffer A, cells were rinsed with PBS and incubated with 10 μM forskolin in the presence of 5 nM serotonin (5-HT) (see Fig. 8 *B*) or a range of concentrations of 5-HT (see Fig. 9 *B*) at 37°C for 30 min in serum-free medium. The phosphodiesterase inhibitor IBMX (50 μM) was present during this treatment. After this incubation, cells were lysed in 10 mM Tris and 5 mM EDTA, pH 7.4 buffer. Cell lysates were boiled for 7–8 min and spun for 15 min in a Sorvall (Newtown, CT) RC-5B centrifuge using a SS-34 rotor to remove precipitated proteins. cAMP amounts in an aliquot of the supernatant were estimated using the [^{3}H]cAMP assay, which is based on the protein-binding method described previously (22). The efficiency of the ligand-mediated reduction in cAMP levels was calculated after normalization of the data to the cAMP content in cells stimulated with forskolin. To determine the IC_{50} of ligand-induced reduction in cAMP, data with a range of concentrations of 5-HT were fitted to the four-parameter logistic equation (Eq. 1), as mentioned earlier, with a few parameters redefined as below:

$$C = a/(1 + (x/I)^s) + b, \tag{1b}$$

where C is the cAMP level normalized to the level of cAMP in cells stimulated with 10 μM forskolin, x denotes the concentration of 5-HT, a is the range (y_{max}–y_{min}) of the fitted curve on the ordinate (y axis), I is the IC_{50} concentration of 5-HT for half-maximal reduction of cAMP, b is the background of the fitted curve (y_{min}), and s is the slope factor.

Phalloidin labeling of F-actin and confocal microscopy

CHO cells stably expressing 5-HT$_{1A}$R-EYFP were plated at a density of 10^4 cells on glass coverslips and were grown in D-MEM/F-12 medium for 48 h. The coverslips were washed with buffer A, and cells were treated with specified amounts of CD for 30 min at room temperature. In other cases, treatment of cells with CD was followed by a 30-min treatment with 10 μM forskolin. After treatment, cells were washed with buffer A and fixed with 3.5% (v/v) formaldehyde for 10 min. Subsequent permeabilization of cells was carried out in the presence of 0.5% (v/v) Triton X-100 and 0.05% (v/v) Tween-20 for 6 min. Cells were washed and stained with rhodamine-phalloidin for 1 h before mounting. Images were acquired on an inverted Zeiss LSM 510 Meta confocal microscope (Jena, Germany) with a 63×, 1.4 numerical aperture oil immersion objective, 108 μm pinhole using the 543 nm line of an argon laser for excitation, and 560 nm long pass filter for the collection of rhodamine fluorescence, giving a fixed z slice of 0.3 μm. The images shown in Fig. 1 represent individual sections from the base (attached to the coverslip) and about ~1 μm (three sections) away from the base into the cell, and the projection of five sections from the base are shown in Fig. 7.

FRAP measurements and analysis

FRAP experiments were carried out on cells that were grown in D-MEM/F-12 medium for 48 h on Lab-Tek chambered coverglass (Nunc, Denmark). Cells were treated with different concentrations of CD in buffer A. In other cases, treatment of cells with CD for 30 min was followed by a 30 min treatment with 10 μM forskolin in buffer A. Experiments were carried out within 20–30 min after addition of CD (and forskolin, wherever needed). Images were acquired at room temperature (~23°C), on an inverted Zeiss LSM 510 Meta confocal microscope, with a 63×, 1.2 numerical aperture water immersion objective using the 514 nm line of an argon laser and 535–590 nm filter for the collection of EYFP fluorescence. Images were recorded with a pinhole of 225 μm, giving a z slice of 1.7 μm. The distinct membrane fluorescence of the cell periphery was targeted for bleaching and monitoring of fluorescence recovery (23,24). Analysis with a control ROI drawn at a certain distance away from the bleach ROI indicated no significant bleach while fluorescence recovery was monitored. Data representing the mean fluorescence intensity of the bleached ROI (~1.4 μm) were background subtracted using a ROI placed outside the cell. Fluorescence recovery plots with fluorescence intensities normalized to prebleach intensities were analyzed on the basis of a modified one-dimensional diffusion equation (25):

$$F_t = (F_i - F_o) \times [1 - \mathrm{erf}\{d/(2 \times (2 \times (D \times t)^{0.5}))\}] + F_o, \tag{2}$$

where F_t is the fluorescence at time t, F_i is the final intensity upon recovery over the period of the experiment, F_o is the intensity immediately after

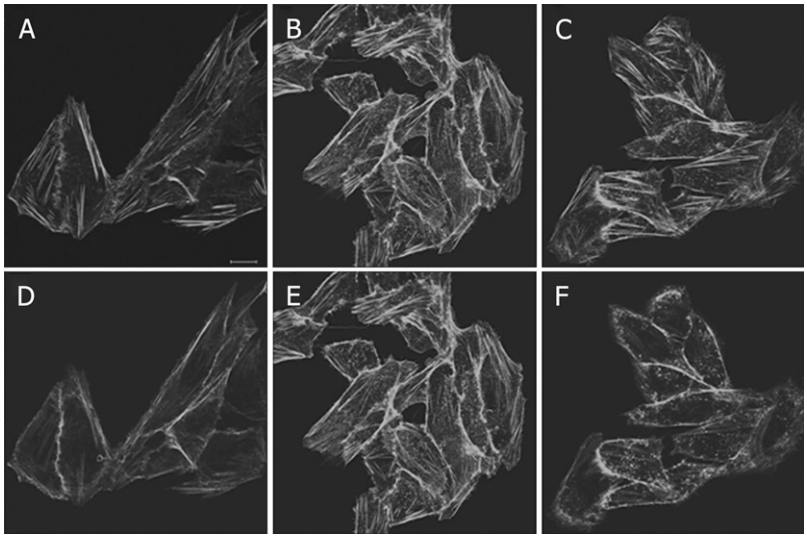

FIGURE 1 Organization of the actin cytoskeleton treated with increasing concentrations of CD. CHO-5-HT$_{1A}$R-EYFP cells cultured in monolayers on coverslips were fixed, and the actin cytoskeleton was stained with rhodamine-phalloidin after treatment with CD in buffer A for 30 min. (*A*) Representative sections at the base (attached to the coverslip) for control (untreated) cells. (*B* and *C*) Cells treated with 0.1 (*B*) and 5 (*C*) μM CD. (*D–F*) For the same fields, sections ~1 μm away from the attached membrane into the cell. Loss of F-actin filaments and formation of F-actin aggregates can be observed (more pronounced in *D–F*) with increasing concentrations of CD treatment. The scale bar represents 10 μm. See Materials and Methods for other details.

bleach, *erf* is the error function, d is the length of the ROI selected for the bleach, and D is the D_{app}. The mobile fraction was estimated as

$$R = (F_i - F_o)/(1 - F_o). \quad (3)$$

Normalized intensities of each data set were fitted individually to Eq. 2, and parameters derived were used in Eq. 3. Statistical analysis was performed on the entire set of derived parameters for all given conditions. Importantly, analysis of fluorescence recovery kinetics based on a two-dimensional diffusion model (26) exhibited a similar trend as that reported here using a one-dimensional diffusion model.

Nonlinear curve fitting and statistical analysis

Nonlinear curve fitting of the fluorescence recovery data to Eq. 2 was carried out using the Graphpad Prism software version 4.00 (San Diego, CA). The correlation between reduction of cAMP levels and the mobile fraction of receptors was plotted with the same software with traces for the 95% confidence band of the regression line (see Fig. 10). Frequency distribution plot and analysis was performed using Microcal Origin software, version 5.0 (OriginLab, Northampton, MA). Plots of data obtained for radioligand binding and fits to Eqs. 1 and 1′ were done with the GRAFIT program, version 3.09b (Erithacus Software, Surrey, UK).

RESULTS

Increasing concentrations of CD lead to gradual loss of F-actin in CHO-5-HT$_{1A}$R-EYFP cells

Cytochalasins are potent inhibitors of actin polymerization in cells. In vitro studies have suggested that CD severs polymerized actin by predominantly binding to the barbed (fast growing) end of the actin filament, thereby shifting the equilibrium toward depolymerization (27). The mechanism of action in vivo, however, appears to be a combination of the above effect of the drug and a secondary cellular response, leading to intensive disruption of the actin cytoskeletal network (28). To monitor the effect of increasing concentrations of CD on the actin cytoskeleton organization in CHO-5-HT$_{1A}$R-EYFP cells, fluorescence images of the actin cytoskeleton stained with rhodamine-phalloidin were obtained by confocal microscopy (Fig. 1). Since FRAP measurements require a clear identification of the plasma membrane, we chose to use an optimal concentration range of CD where the cellular morphology would remain more or less intact. We also optimized the period of treatment such that for the maximal concentration of CD used (5 μM CD), the cellular morphology is retained over the time of measurement.

With increasing CD concentration, a progressive disintegration of actin filaments was observed along with the appearance of small F-actin aggregates. The changes observed at the base (attached to the coverslip) are relatively less although small F-actin aggregates begin to appear (Fig. 1, *A–C*). Individual sections of the same field $\sim$1 μm into the cells exhibit more pronounced effects of CD treatment and are shown in Fig. 1, *D–F*. As can be seen in Fig. 1, although untreated cells do not show any F-actin disintegration, treatment with 5 μM CD led to a drastic shortening of the actin filaments accompanied by the formation of large focal aggregates of F-actin (Fig. 1 *F*). Further quantitation of the CD effect from these images is difficult due to the fact that the images presented represent selected sections of a z stack of the field (as mentioned in Materials and Methods). Moreover, treatment with CD results in fragmentation of actin filaments into smaller F-actin aggregates, which appear brighter under a fluorescence microscope, rendering intensity-based analysis unsuitable. It should be noted that the action of CD on cells was fast, and changes in cellular morphology were visible within minutes for higher concentrations of CD.

5-HT$_{1A}$R-EYFP exhibits actin cytoskeleton-dependent dynamics in the plasma membrane

The lateral dynamics of 5-HT$_{1A}$R-EYFP in plasma membranes was studied using FRAP. Representative images corresponding to the FRAP measurement are shown in Fig. 2. The cellular periphery with clear plasma membrane localization of 5-HT$_{1A}$R-EYFP was targeted for FRAP experiments (23,24). This particular selection of geometry not only reduces the interference in recovery from intracellular 5-HT$_{1A}$R-EYFP but also reduces the diffusion problem predominantly to one dimension. An extensive data set was collected to take into account statistical variation inherent in the analysis of dynamics of molecules in membranes (Tables 1 and 2). Frequency distribution histograms of diffusion coefficients and mobile fractions are shown in Figs. 3 and 4. One-component Gaussian fit to the histograms gave a reduced $\chi^2 < 0.002$ and < 0.0005 for the diffusion coefficient and mobile fraction, under all conditions of treatment. This indicates the presence of a predominantly single mobile population in the spatiotemporal scale of the measurement. The D_{app} of 5-HT$_{1A}$R-EYFP was in the range of 0.14–0.15 $\mu m^2 s^{-1}$ and did not exhibit any significant change upon cytoskeletal destabilization (Fig. 5 *A*). Importantly, we observed a progressive increase in the mobile fraction of receptors with increasing concentration of CD. Upon treatment with 5 μM CD, the mobile fraction showed an increase of

TABLE 1 D_{app} and mobile fractions of 5-HT$_{1A}$R-EYFP: CD treatment

Experimental condition	D_{app} (μm^2 s^{-1}) mean ± SE	The mobile fraction (%) mean ± SE	N p-value (for mobile fraction)	
Control (0 μM CD)	0.138 (± 0.004)	73.95 (± 0.78)	148	-
0.1 μM CD	0.141 (± 0.006)	75.17 (± 1.02)	84	NS
0.5 μM CD	0.152 (± 0.007)	77.19 (± 1.41)	41	NS
1 μM CD	0.135 (± 0.008)	78.68 (± 1.34)	50	<0.01
2 μM CD	0.137 (± 0.005)	80.39 (± 1.26)	50	<0.001
5 μM CD	0.15 (± 0.008)	84.11 (± 1.27)	50	<0.0001

Two-tailed, unpaired Student's t-test was performed on the mobile fraction values, and the corresponding p-values are shown. Differences in D_{app} were found to be not significantly different. N represents the number of independent measurements. NS denotes not significant. See Materials and Methods for other details.

TABLE 2 D_{app} and mobile fractions of 5-HT$_{1A}$R-EYFP: Forskolin and CD treatment

Experimental condition	D_{app} (μm^2 s^{-1}) mean ± SE	The mobile fraction mean ± SE (%)	N	p-value (for mobile fraction)
Fsk	0.127 (± 0.005)	78.16 (± 1.66)	30	<0.05
Fsk + 0.2 μM CD	0.155 (± 0.007)	74.52 (± 0.98)	32	NS
Fsk + 0.5 μM CD	0.147 (± 0.007)	75.58 (± 1.52)	33	NS
Fsk + 1 μM CD	0.155 (± 0.009)	77.11 (± 1.38)	36	NS
Fsk + 2 μM CD	0.143 (± 0.006)	79.05 (± 1.78)	32	<0.01
Fsk + 5 μM CD	0.141 (± 0.006)	82.45 (± 1.18)	34	<0.0001

Two-tailed, unpaired Student's t-test was performed on the mobile fraction values, and the corresponding p-values are shown. Differences in D_{app} were found to be not significantly different. N represents the number of independent measurements. For forskolin (Fsk) treatment, the differences in the mobile fraction were tested against values obtained with control (no treatment). NS denotes not significant. See Materials and Methods for other details.

~10% relative to control cells (Tables 1 and 2 and Fig. 5 *B*). We found it difficult to perform FRAP measurements on cells treated with higher concentrations of CD due to rapid loss of cellular morphology under those conditions, which made selecting plasma membranes for FRAP measurements difficult.

The increase in the mobile fraction suggests that F-actin destabilization leads to an increase in the fraction of receptors, which are freely mobile. This implies that an intact actin cytoskeleton is an essential regulator of the fraction of mobile receptors. These numbers assume relevance in light of a recent report on simulation of FRAP measurements for molecules undergoing diffusion on a membrane with ''rafts'' and ''actin-fences'', in which a maximal change of ~10% in the mobile fraction was observed between conditions of the presence and absence of actin-fences (29). More importantly, these authors observed no significant change in diffusion coefficients under such conditions, similar to our observations (Fig. 5 *A*). Although our data does not permit us to comment on the presence of membrane rafts, these results appear to be in excellent agreement with the simulated results for the picket fence model of membrane skeleton. To the best of our knowledge, this is the first report implying a dependence of the mobility of the serotonin$_{1A}$ receptor and the actin cytoskeleton.

Actin cytoskeleton reorganization induced by the elevation of intracellular cAMP level affects the dynamics of 5-HT$_{1A}$R-EYFP

Since actin cytoskeleton destabilization upon CD treatment increased the mobile fraction of the receptors, we tested whether the effect on the mobility of the receptor can be brought about by agents other than those that directly interfere with the actin cytoskeleton. An increase in the intracellular levels of cAMP has been known to induce significant changes in the cellular architecture of fibroblasts and neuronal cells (30,31). Increased cAMP levels in cells lead to dissolution of stress fibers and the induction of stellate morphology in neuronal cells. Elevation of cAMP levels has been suggested to activate PKA, which results in inhibition of RhoA, a

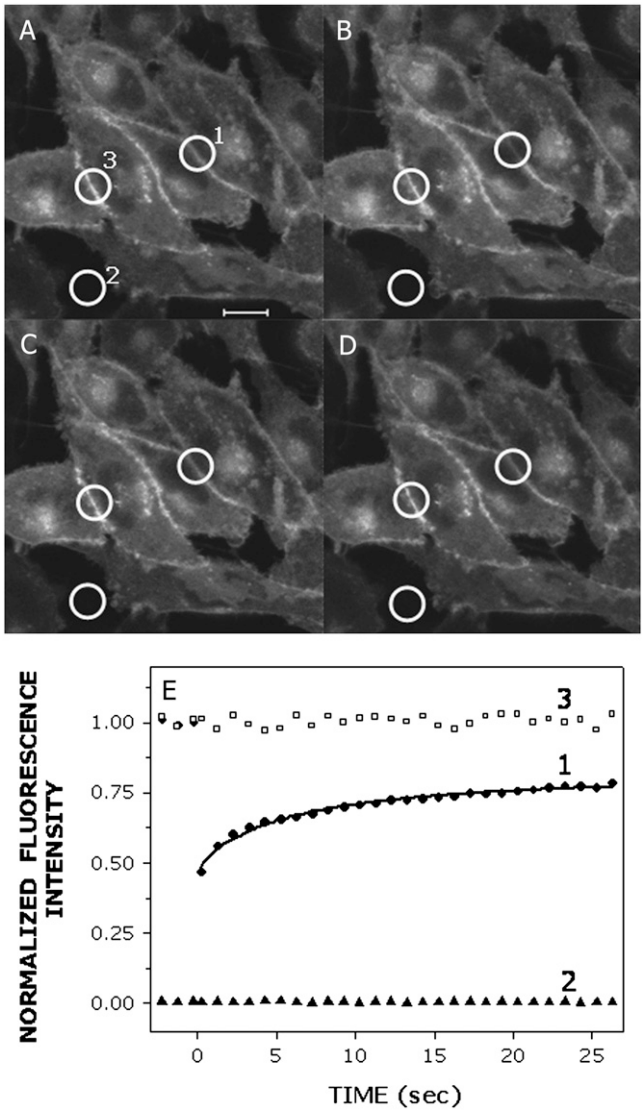

FIGURE 2 Analysis of the recovery of fluorescence intensity after photobleaching of 5-HT$_{1A}$REYFP. The cellular periphery with clear plasma membrane localization of 5-HT$_{1A}$R-EYFP was targeted for FRAP experiments. Typical images corresponding to prebleach (*A*), bleach (*B*), immediate postbleach (*C*), and complete (*D*) recovery. The plot in *E* shows a representative set of normalized fluorescence intensity of 5-HT$_{1A}$REYFP (●) corresponding to region 1, and normalized background intensity (▲), corresponding to region 2. The normalized fluorescence intensity in control region 3 (□) was monitored for the same time period and plotted in *E*, showing no significant photobleaching of the region due to repeated scanning. The dimensions of the regions are only representative. The bold solid line tracing the recovery is the fit of the data to Eq. 2. The scale bar represents 10 μm. See Materials and Methods for details.

GTPase actively involved in actin filament dynamics and myosin phosphorylation (32). As shown in Fig. 7 *D*, treatment of CHO-5-HT$_{1A}$R-EYFP cells with 10 μM forskolin, which elevates intracellular cAMP levels by activating AC, leads to a significant reorganization of the actin cytoskeleton.

We observed shrinkage of cells and ruffle-like formations along the cell periphery, with an overall reduction in F-actin

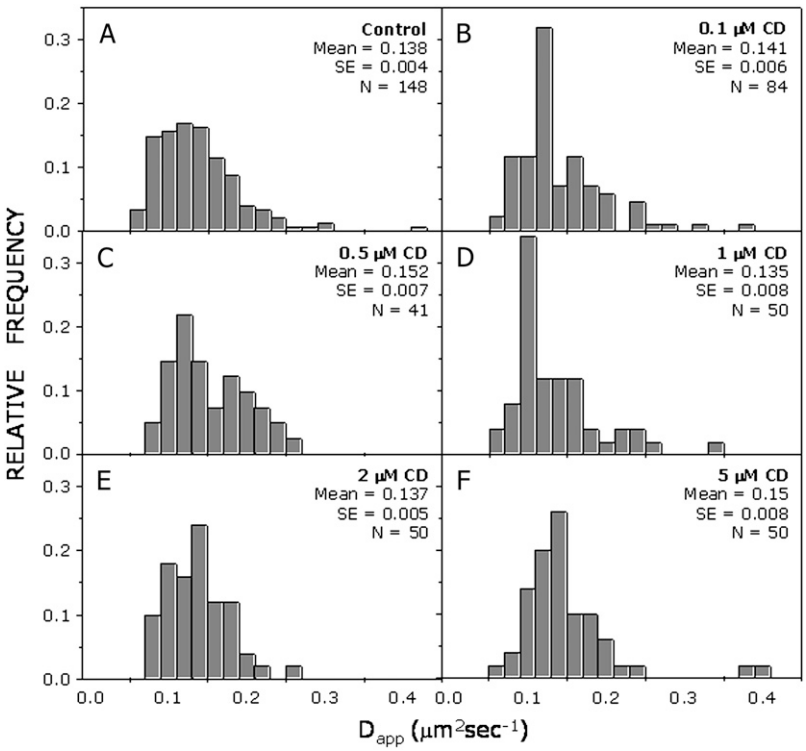

FIGURE 3 Frequency distribution histograms of the D_{app} of 5-HT_{1A}R-EYFP determined by FRAP. D_{app} was derived by fitting the normalized recovery data to Eq. 2. (*A*) Data for control (untreated) cells. (*B–F*) 0.1 (*B*), 0.5 (*C*), 1 (*D*), 2 (*E*), and 5 (*F*) μM CD. The means $\pm$ SE are shown in all cases. *N* represents the number of independent experiments performed in each case. Note that the distribution of D_{app} remains unimodal in all cases, indicating the existence of a single population of mobile receptors. See Tables 1 and 2 and Materials and Methods for other details.

staining upon forskolin treatment. It must be noted that the changes induced by forskolin treatment on the actin cytoskeleton were different from the changes observed upon CD treatment. Almost no F-actin aggregates were observed with forskolin treatment, as is generally observed for treatment with CD (see Fig. 7, *B–D*). This may be due to the differences in the mechanisms of the two treatments. As described earlier, CD binding to actin filaments shifts the equilibrium toward depolymerization, thereby predominantly affecting the previously polymerized filaments. Elevation of intracellular cAMP, on the other hand, affects the cytoskeleton by deactivating proteins involved in actin dynamics whose effect

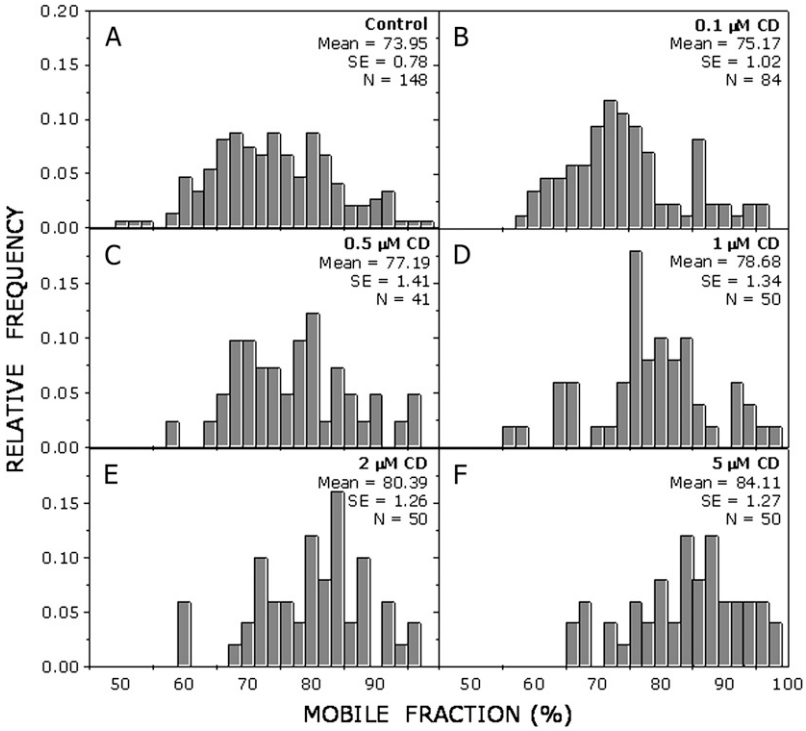

FIGURE 4 Frequency distribution histograms of the mobile fraction of 5-HT_{1A}R-EYFP determined by FRAP. The mobile fraction was obtained from Eq. 3, utilizing the fitted parameters from Eq. 2. (*A*) Data for control (untreated) cells. (*B–F*) 0.1 (*B*), 0.5 (*C*), 1 (*D*), 2 (*E*), and 5 (*F*) μM CD. The means $\pm$ SE are shown in all cases. *N* represents the number of independent experiments performed in each case. Note that although the distribution of the mobile fraction remains unimodal in all cases, there is a significant shift toward higher values upon treatment with increasing concentrations of CD. See text and Tables 1 and 2 for details.

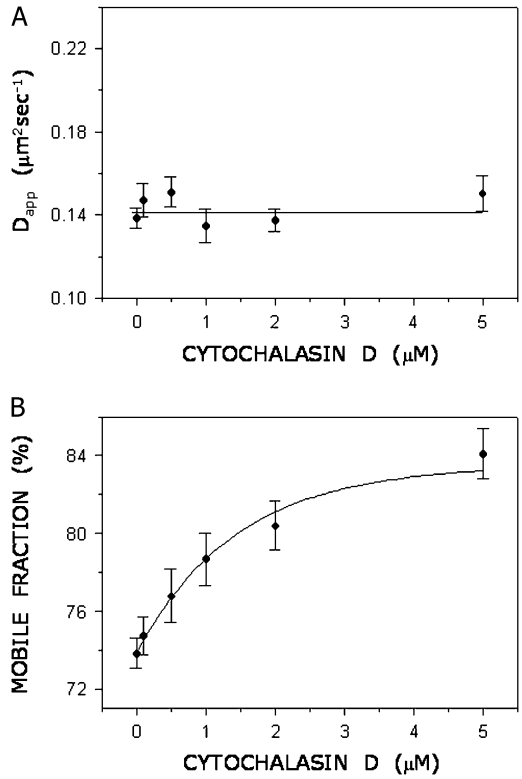

FIGURE 5 Lateral mobility of 5-HT$_{1A}$R-EYFP. (*A*) D_{app} of the receptor upon treatment with increasing concentrations of CD; (*B*) Change in the mobile fraction of the receptor under the same conditions as in (*A*). The data points represent means ± SE of *N* independent experiments corresponding to Figs. 3 and 4. The lines drawn are mere guides to the eye. See Tables 1 and 2 and Results for details.

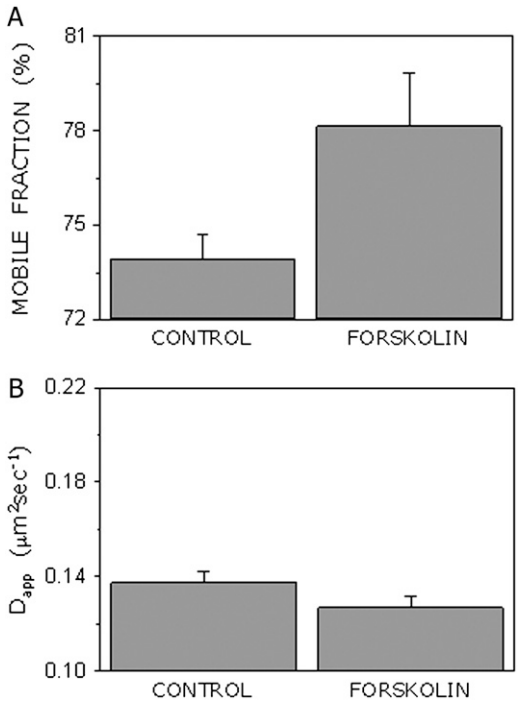

FIGURE 6 The effect of elevation of intracellular cAMP on 5-HT$_{1A}$R-EYFP mobility. The (*A*) the mobile fraction and (*B*) D_{app} of 5-HT$_{1A}$R-EYFP in the absence (control) and presence of 10 μM forskolin. Data represent means ± SE for 30 independent measurements. See Tables 1 and 2 and Results for details.

on the preformed filaments may be lower than that on the formation of new filaments. Nevertheless, we observe an increase in the mobile fraction of receptors upon treatment with forskolin, consistent with the loss of the actin cytoskeleton (Fig. 6 *A*). The D_{app} of the receptor remained more or less invariant under this condition (Fig. 6 *B*). The increase in the mobile fraction of the receptor upon actin reorganization by an independent mechanism reinforces the fact that the mobility of the serotonin$_{1A}$ receptor is regulated by the actin cytoskeleton.

Actin destabilization leads to increased signaling mediated by 5-HT$_{1A}$R-EYFP

Since the serotonin$_{1A}$ receptor is coupled to the $G_{\alpha i}$ subunit, it is expected to reduce intracellular cAMP levels upon ligand-mediated activation. To assess the effect of altered dynamics of the receptor due to actin destabilization on its signaling efficiency, we estimated the extent to which the receptor would reduce cAMP levels upon stimulation by serotonin. A complication arises due to the fact that the basal levels of cAMP are inappropriate to measure this signaling. The cellular cAMP level, therefore, needs to be elevated (with agents such as forskolin) for the estimation of $G_{\alpha i}$-mediated signaling. As described earlier, an elevation of the intracellular level of cAMP induces significant reorganization of the actin cytoskeleton and also alters the mobility of the serotonin$_{1A}$ receptor. Interestingly, pretreatment of cells with CD appears to considerably reduce the effect of forskolin treatment on the actin cytoskeleton. As shown in Fig. 7, initial treatment of cells with as low as 0.1 μM CD followed by forskolin (10 μM) treatment does not exhibit the changes observed when cells were treated with only forskolin (*D* and *E*). Although we observed an overall reduction of F-actin staining in all cases where forskolin was used, the presence of CD appears to reduce this effect. Fig. 8 *A* shows the mobile fractions obtained in the presence of forskolin for cells pretreated with increasing CD concentrations. As can be observed, the mobile fraction of the receptor showed a similar trend when only CD was used in increasing concentrations. The D_{app} in all cases remained largely invariant (not shown).

The loss of the effect of forskolin upon pretreatment with CD has been reported previously. This effect was explained as a possible consequence of the drugs sharing a common inhibitory mechanism of action (33). It has been further suggested that a possible mechanism of the action of CD may require a functional PKA (34). Considering the fact that PKA is a necessary component of cAMP-mediated signaling, it is likely that pretreatment with CD alters the available levels of PKA, thereby modifying the effect of cAMP-dependent changes in the actin cytoskeleton. Importantly, we observed

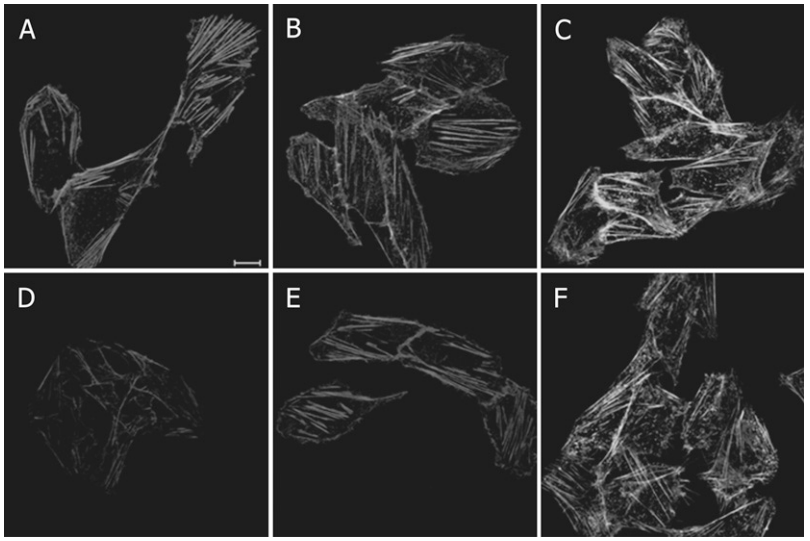

FIGURE 7 Organization of the actin cytoskeleton of CHO-5-HT_{1A}R-EYFP cells, observed by staining with rhodamine-phalloidin, subsequent to treatments as mentioned below: (*A*) control (untreated) cells; (*B*) treated with 0.1 μM CD for 30 min; (*C*) treated with 5 μM CD for 30 min; (*D*) treated with 10 μM forskolin for 30 min; (*E*) treated with 10 μM forskolin for 30 min, subsequent to treatment with 0.1 μM CD for 30 min; (*F*) treated with 10 μM forskolin for 30 min, subsequent to treatment with 5 μM CD for 30 min. The scale bar represents 10 μm. See Materials and Methods for other details.

that pretreatment with even a relatively small concentration of CD (0.1 μM) is sufficient to reduce the effect of 10 μM forskolin. For the estimation of signaling of the receptor, forskolin was hence used in all cases as an agent that can elevate the basal cellular cAMP levels. Subsequent reduction in cAMP levels, upon stimulation with serotonin, was estimated as a measure of the efficiency of signaling by the receptor. It is important to note here that the control for signaling measurements were cells which were not treated with CD, and so in these cases we observe the effect of forskolin itself. The concentration of serotonin (5 nM) chosen for the measurement of signaling efficiency was IC_{50} in control cells (not treated with CD). For these experiments, cells pretreated with different concentrations of CD were incubated in the presence of forskolin (10 μM) and serotonin (5 nM). The relative reduction in cAMP level, normalized to that found upon forskolin stimulation alone (without addition of serotonin), is shown in Fig. 8 *B*. As can be seen, the reduction in cAMP levels, mediated by the receptor, shows an increase upon treatment with increasing concentrations of CD. Significantly, the mobile fractions and the reduction in cAMP level, exhibited very similar trends with increasing CD treatment (evident upon comparison of Fig. 8, *A* and *B*; see also Tables 1 and 2). To rule out the possibility that CD treatment itself could lead to the regulation of AC, we estimated the level of basal cAMP present in cells pretreated with CD.

The amount of cAMP estimated under different conditions is shown in Fig. 9 *A*. No significant difference was observed in the basal cAMP levels between control and CD-treated cells, indicating that CD treatment does not lead to the stimulation or inhibition of AC. If the levels of cAMP are brought down to different extents due to treatment with varying CD concentrations (Fig. 8 *B*), IC_{50} of reduction by serotonin, in principle, should also shift. To assess the change in IC_{50} of signaling for a given concentration of CD, we estimated the effective reduction in cAMP levels over a range of serotonin concentrations. As shown in Fig. 9 *B*, the IC_{50} of signaling for 0.2 μM CD-treated cells (42.8 nM) was about an order of magnitude higher compared to the corresponding value (5.8 nM) for control cells (not treated with CD but in the presence of forskolin) and for cells treated with 5 μM CD (6.2 nM). This implies that signaling is more efficient under conditions of actin destabilization.

Increased mobility of 5-HT_{1A}R-EYFP correlates strongly to its efficiency in signaling

A plot of the mobile fractions of the receptor versus the efficiency in reduction of cAMP levels, generated by using data from Fig. 8, *A* and *B*, is shown in Fig. 10. A linear regression analysis between the mobile fraction and signaling produced a positive correlation of ~0.95. The 95% confidence intervals contained all the data points, implying a significant relationship between the two parameters observed. Such a correlation between the mobile fraction of the receptor and its signaling implies a fundamental physical basis of signaling. The fact that a strong correlation is observed despite the natural variation of the system, both in terms of mobility and signaling, reinforces the point.

Ligand binding of 5-HT_{1A}R-EYFP remains unaltered upon CD treatment

Since receptor stimulation in the case of GPCRs involves multiple steps, the increased efficiency of signaling may be due to the fact that the binding of the receptor toward its agonist is altered upon cytoskeletal destabilization. To monitor this, we performed radioligand binding assay of the receptor in membranes prepared from CD-treated cells. Previous work from our laboratory has established that the agonist preferentially binds to receptors which are coupled to G-proteins, whereas the antagonist binds to both G-protein coupled and uncoupled receptors (35). Fig. 11 shows that both the agonist ([^{3}H]8-OH-DPAT) and antagonist

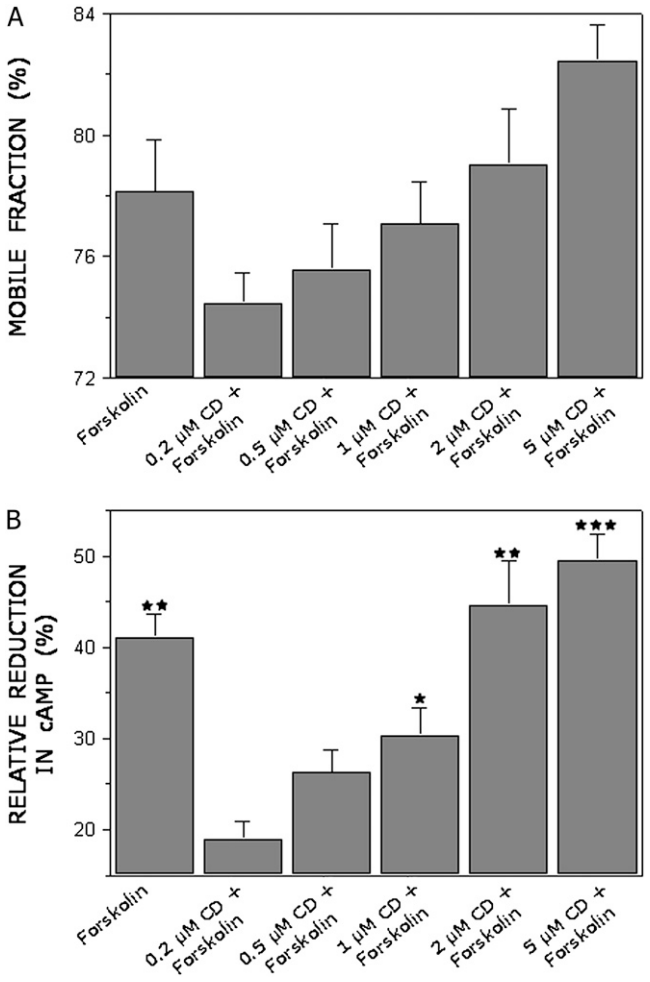

FIGURE 8 The mobile fraction and signaling of 5-HT$_{1A}$R-EYFP under different conditions of actin destabilization. (*A*) The mobile fraction of 5-HT$_{1A}$R-EYFP in the presence of 10 μM forskolin subsequent to treatment with increasing concentrations of CD. Data represent means ± SE for at least 30 independent experiments. (*B*) The relative reduction in forskolin-stimulated (forskolin concentration 10 μM) levels of cAMP in CHO-5-HT$_{1A}$R-EYFP cells upon activation by 5 nM serotonin, subsequent to treatment with increasing concentrations of CD. Data represent means ± SE for at least three independent experiments (*, **, and *** correspond to p-values < 0.05, 0.01, and 0.001, respectively; the differences in relative reduction in cAMP were tested against the corresponding value obtained with 0.2 μM CD + forskolin). See text and Tables 1 and 2 for other details.

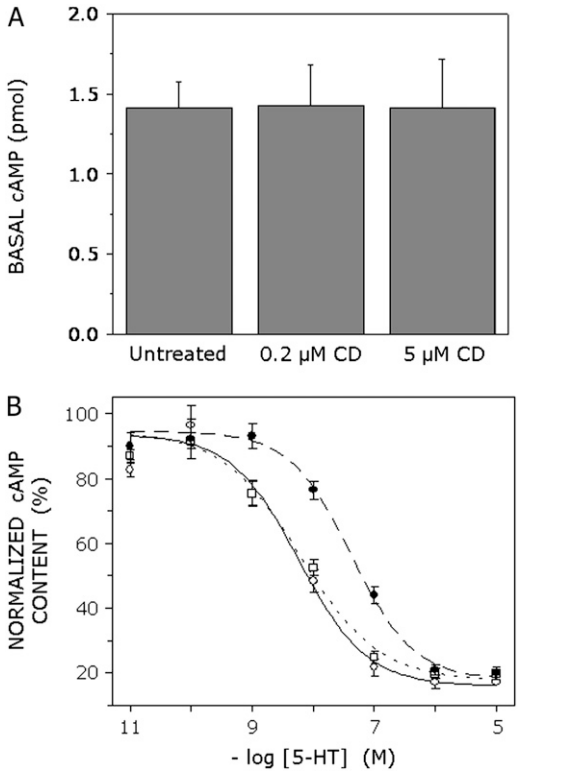

FIGURE 9 Estimation of cAMP under conditions of actin destabilization. (*A*) The basal level of cAMP in an aliquot of cell lysate upon treatment with 0.2 and 5 μM CD. The basal cAMP level in untreated cells is also shown. The data points represent means ± SE of at least three independent experiments. (*B*) The effect of CD treatment on IC$_{50}$ of relative reduction in cAMP: control (untreated) cells (○, —), cells treated with 0.2 (●, – –), and 5 (□,—) μM CD were stimulated with a range of concentrations of serotonin (5-HT). The amount of cAMP measured was normalized to levels of cAMP in cells treated with forskolin (in the absence of any added CD or serotonin). The concentration of forskolin used was 10 μM. The curves are nonlinear regression fits to Eq. 1′. The data points represent means ± SE of three independent experiments. See Materials and Methods for other details.

([^{3}H]*p*-MPPF) binding remained essentially invariant upon CD treatment, irrespective of the concentration of CD used.

G-protein coupling of 5-HT$_{1A}$R-EYFP remains unaffected upon actin cytoskeleton destabilization

The coupling of the receptor to G-proteins represents an important aspect in signaling mediated GPCRs. Signaling mediated by the receptor is dependent on its coupling to the respective G-protein. To check whether the increased efficiency in signaling upon cytoskeletal destabilization is due to an increased coupling of the receptor to the G-protein, we examined the sensitivity of agonist binding in the presence of various concentrations of GTP-γ-S, a nonhydrolyzable analog of GTP. We have previously shown that agonist binding to serotonin$_{1A}$ receptors displays sensitivity to agents such as GTP-γ-S that uncouple the normal cycle of guanine nucleotide exchange at the G_α subunit caused by receptor activation (35). The specific binding of the agonist to serotonin$_{1A}$ receptors is thus sensitive to guanine nucleotides and is inhibited with increasing concentrations of GTP-γ-S. In the presence of GTP-γ-S, serotonin$_{1A}$ receptors undergo an affinity transition, from a high affinity G-protein coupled to a low affinity G-protein uncoupled state (35). In agreement with these results, Fig. 12 shows a characteristic reduction in binding of the agonist [^{3}H]8-OH-DPAT in the presence of increasing concentrations of GTP-γ-S with an estimated IC$_{50}$ of 0.97 nM (control). The corresponding value in the case of CD-treated membranes is ~1.08 nM, irrespective of the CD concentration used. This shows that there is no significant change in G-protein coupling upon cytoskeletal destabilization.

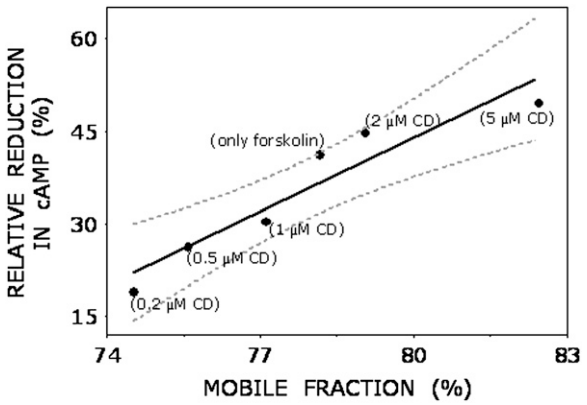

FIGURE 10 Correlation of 5-HT_{1A}R-EYFP the mobile fraction and serotonin-mediated relative reduction in cAMP. Data plotted are from Fig. 8, *A* and *B*. The concentration of serotonin used was 5 nM. Linear regression analysis gave a correlation coefficient, $r \sim 0.95$. The 95% confidence band is plotted as dashed lines to indicate the significance of the correlation.

DISCUSSION

Understanding cellular signaling by membrane receptors in terms of their lateral dynamics represents a challenging area in biology. Considering the fact that about one half of all genetically encoded proteins in the eukaryotic genome are membrane-associated proteins, it is likely that ~50% of all reactions occurring in a cell occur on membranes (36). Since a majority of all membrane proteins are targeted to the plasma membrane, a significant fraction of cellular reactions occur on or close to the plasma membrane. The plasma membrane accordingly not only acts as a selective barrier for the cell but also serves as a platform for the initiation and regulation of signaling pathways. It is therefore relevant to understand the mechanism of processes involved in signaling on the membrane for a proper understanding of cellular function. In this work, we explored the relationship between the actin cytoskeleton-dependent lateral mobility of the G-protein-coupled $serotonin_{1A}$ receptor and its signaling.

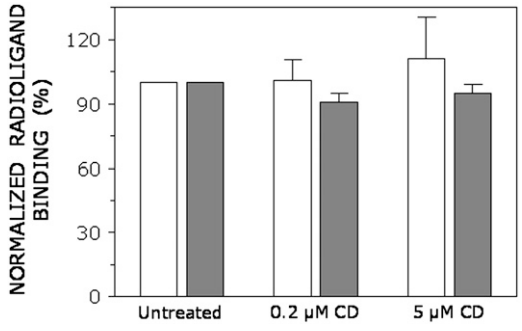

FIGURE 11 Specific binding of the agonist [^{3}H]8-OH-DPAT (*open bars*) and antagonist [^{3}H]*p*-MPPF (*solid bars*) to membranes isolated from CHO-5-HT_{1A}R-EYFP cells treated with 0.2 or 5 μM CD for 30 min. Values are expressed as percentages of specific radioligand binding obtained in membranes isolated from untreated cells. Data represent means ± SE of duplicate points from at least six independent experiments. See Materials and Methods for other details.

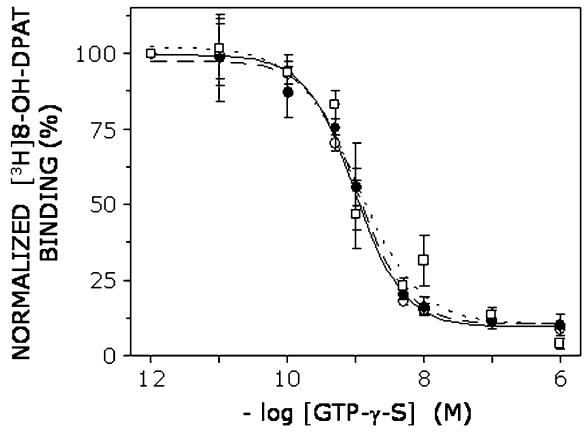

FIGURE 12 Effect of increasing concentrations of GTP-γ-S on specific binding of [^{3}H]8-OH-DPAT to 5-HT_{1A}R-EYFP in membranes isolated from untreated cells (○, —) and cells treated with 0.2 (●, – –), or 5 (□,—) μM CD. Values are expressed as percentages of specific [^{3}H]8-OH-DPAT binding in the presence of 10^{-12} M GTP-γ-S in each case. The curves shown are nonlinear regression fits to the experimental data using Eq. 1. Data represent means ± SE of four independent experiments. See Materials and Methods for other details.

Although the theoretical framework for lateral diffusion in membranes was described a number of years back (37), models for lateral diffusion of membrane-bound molecules continue to emerge (38). In normal Brownian diffusion, the mean-square displacement of the molecule is linearly proportional to time. However, the mean-square displacement of molecules on membranes has been reported to be non-Brownian in many cases, particularly when monitored at varying timescales (39). Such diffusion behavior has been termed ''anomalous diffusion''. Diffusion of molecules on cellular membranes is likely to be hindered due to cytoskeleton and other interacting components, leading to anomalous diffusion. Interestingly, it appears that the nature of diffusion observed is related to the timescale of measurement (39). It should be mentioned here that for FRAP measurements performed on the characteristic timescale of the order of seconds to minutes, it is difficult to resolve anomalous from normal diffusion (40). Our results show that with increasing destabilization of the actin cytoskeleton, there is a gradual increase in the mobile fraction of the $serotonin_{1A}$ receptor, whereas the D_{app} does not exhibit any significant change. The values obtained for the D_{app} are in the range of 0.14–0.15 $\mu m^2\ s^{-1}$, similar to values reported for GPCRs from FRAP measurements in CHO cells (24,41,42). The increase in the mobile fraction with increasing cytoskeletal destabilization can, then, be due to the gradual release of receptors, previously confined by the actin network. An alternative explanation of the effect of actin destabilization could be the alteration of membrane lipid organization in membrane domains (''rafts''), leading to the release of the receptors, as reported recently (43–45).

Cellular signaling by GPCRs involves their activation upon binding to ligands present in the extracellular environment and the subsequent transduction of signals to the

interior of the cell through concerted changes in their transmembrane domain structure (46). The major paradigm in this signal transduction process is that stimulation of GPCRs leads to the recruitment and activation of heterotrimeric G-proteins (47). These initial events, fundamental to all types of GPCR signaling, occur at the plasma membrane via protein-protein interactions. An important consequence of this is that the dynamics of the activated receptor on the cell surface represents an important determinant in its encounter with G-proteins and has significant impact on the overall efficiency of the signal transduction process (16). Evidence for this comes from a previous report in which the activation of G-proteins by light-activated rhodopsin was determined by diffusion rates of the receptor in the membrane (48).

In this context, the membrane organization and dynamics of GPCRs and G-proteins participating in this signal transduction process assume relevance. The classical view of receptor/G-protein function in cells proposes free diffusion of molecules on the cell surface such that the probability of such interaction would depend on random collisions (reviewed in Neubig (49)). However, the specific and rapid signaling responses, characteristic of GPCR activation, cannot be explained solely based on a uniform distribution of receptors, G-proteins, and effectors, one or more of which could even be in low abundance, on the cell membrane (50,51). This leads to the possibility that receptor/G-protein interactions may be dependent on their organization in membranes. G-proteins have earlier been shown as largely immobile, and it has been reported that their mobility remains low even after cytoskeleton destabilization (52). Various other studies have suggested a highly organized and consequently restricted distribution of G-proteins in the plasma membrane (49). Interestingly, experimental evidence on the distribution of AC suggests a heterogeneous distribution, where GPCRs, G-proteins, and AC were found in similar membrane fractions (50,53). Spatiotemporal regulation of interactions between receptor, G-proteins, and effectors on the cell membrane by the restriction imposed on their mobility (e.g., by the cytoskeleton) is now believed to be an important determinant in GPCR signaling (51,54,55).

An increase in the mobile fraction of the receptor can be interpreted as an increase in the sampling space of the receptor. Actin destabilization may thus lead to increased probability of interactions of the receptor with its signaling partners in the context of the heterogeneous distribution of the effectors (G-proteins and AC). This is supported by the observation that the change in signaling mediated by the receptor increases in a correlated manner with increase in the mobile fraction (Fig. 10). Interestingly, a similar correlation has previously been observed for the vasopressin V_2-receptor (56). These authors reported that the ability of the vasopressin V_2-receptor to activate AC via G-proteins was directly dependent on the mobile fraction of these receptors on the cell membrane. Jans et al. measured the mobile fraction of the vasopressin V_2-receptor as a function of temperature, and attributed changes in the mobile fraction to temperature-induced actin reorganization. In the case here, we depolymerized the actin cytoskeleton with CD or by elevating intracellular cAMP level and observed a positive correlation of $\sim$0.95 between the mobile fraction and signaling efficiency monitored by reduction in cAMP levels. Our results are therefore in general agreement with the observations of Jans et al. The vasopressin V_2-receptor is a $G_{\alpha s}$-coupled GPCR and activates AC, leading to elevation of cAMP levels in cells. As mentioned earlier, the serotonin$_{1A}$ receptor is coupled to $G_{\alpha i}$ and downregulates AC, thereby lowering cAMP levels. These two subtypes ($G_{\alpha i}$ and $G_{\alpha s}$) of heterotrimeric G-protein are believed to act differently upon activation, e.g., the $G_{\alpha i}$ family of proteins has been reported to undergo subunit rearrangement rather than dissociation upon activation, which is characteristic of the $G_{\alpha s}$ subtype (57). Moreover, whereas Jans et al. monitored the mobility of fluorescent ligand-bound vasopressin V_2-receptors, our results were obtained using receptors with an EYFP tag. Despite these differences in their mode of activation, it is interesting to note that the effect of increased mobility of the receptor resulting in increased efficiency of signaling is observed for both the receptors and appears to be independent of the nature of the G-protein involved. Importantly, we observe that the change in signaling efficiency (as measured by IC_{50} values, Fig. 9 *B*) is different by about an order of magnitude corresponding to a 10% change in mobile fraction. Notably, the change in signaling is more pronounced than the change in mobile fraction. This may be due to the fact that signaling from a single receptor gets amplified manyfold at the cAMP level. We further report that the binding of the receptor to its agonist and its extent of G-protein coupling remain unaltered upon actin destabilization. The lack of significant alteration in ligand binding and G-protein coupling upon CD treatment may be due to the fact that these assays were performed on cell membranes upon pretreatment of cells with CD. It is possible that the process of membrane preparation eliminates any effect of actin cytoskeleton on the receptor. Interestingly, a recent report suggests that membrane fractions isolated from cells are interconnected with the actin cytoskeleton (58).

The possible reason for the observed increase in the mobile fraction upon actin destabilization merits comment. It has been recently reported that the actin-dependent mobility of the cystic fibrosis transmembrane conductance regulator protein is regulated by its C-termini PDZ motif (59). These domains are believed to help anchor transmembrane proteins to the cytoskeleton and hold together signaling complexes. The existence of such a binding motif has recently been reported for a serotonin$_2$-like receptor in *Caenorhabditis elegans* (60). A possible region of the receptor that may interact with PDZ proteins and/or actin is the long third intracellular loop of the receptor, although this needs to be confirmed. This region has previously been shown to bind calmodulin (61), which is known to interact with PDZ proteins (60). However,

to the best of our knowledge, there are no reports in the literature implying the existence of PDZ domains in serotonin$_{1A}$ receptors.

Our results are important in the overall context of the role of actin cytoskeleton in signaling mediated by the serotonin$_{1A}$ receptor in particular and GPCRs in general. In addition, processes involved in neurite growth require extensive restructuring of the actin cytoskeleton. Interestingly, activation of the serotonin$_{1A}$ receptor has been implicated in neurite outgrowth and neuronal survival (12). These results assume significance in light of a recent report that the protein mobilities are different between navigating and nonnavigating growth cones in neurons, possibly due to differences in the organization of the actin cytoskeleton (62). Moreover, with growing evidence in favor of cAMP transducing specific responses by localized signaling (63), our results raise an interesting possibility of a dynamic system involving the actin cytoskeleton, cAMP, and the serotonin$_{1A}$ receptor. We note that the above system, in the presence of extracellular serotonin, could be driven by a local negative feedback loop wherein an increase in local intracellular cAMP level can reorganize the actin cytoskeleton, leading to increased mobility and hence signaling by the serotonin$_{1A}$ receptor, which in effect would reduce the cAMP levels. It is notable that cAMP-dependent neurite outgrowth has been observed earlier (64,65). In light of our results, it may be possible to link serotonin-mediated responses with neurite outgrowth. In summary, our results show that destabilization of the actin cytoskeleton can lead to increased receptor signaling. Whether the effect of increased mobility by serotonin$_{1A}$ receptors during neural growth constitutes a signaling cue represents a fascinating question.

We thank Nandini Rangaraj for help with the confocal microscope, Kaushlendra Tripathi for useful discussion, and members of our laboratory for critically reading the manuscript and for helpful discussion and suggestions.

This work was supported by the Council of Scientific and Industrial Research (CSIR), Government of India. S.G. thanks CSIR for the award of a research fellowship. T.J.P. thanks the National Brain Research Center for the award of a postdoctoral fellowship. A.C. is an Honorary Professor of the Jawaharlal Nehru Centre for Advanced Scientific Research, Bangalore (India).

REFERENCES

1. Mukherjee, S., and F. R. Maxfield. 2004. Membrane domains. *Annu. Rev. Cell Dev. Biol.* 20:839–866.
2. Kusumi, A., and K. Suzuki. 2005. Toward understanding the dynamics of membrane-raft-based molecular interactions. *Biochim. Biophys. Acta.* 1746:234–251.
3. Marguet, D., P.-F. Lenne, H. Rigneault, and H.-T. He. 2006. Dynamics in the plasma membrane: how to combine fluidity and order. *EMBO J.* 25:3446–3457.
4. Jacobson, K., O. G. Mouritsen, and R. G. W. Anderson. 2007. Lipid rafts: at a crossroad between cell biology and physics. *Nat. Cell Biol.* 9:7–14.
5. Fredriksson, R., M. C. Lagerström, L.-G. Lundin, and H. B. Schiöth. 2003. The G-protein-coupled receptors in the human genome form five main families. Phylogenetic analysis, paralogon groups, and fingerprints. *Mol. Pharmacol.* 63:1256–1272.
6. Pierce, K. L., R. T. Premont, and R. J. Lefkowitz. 2002. Seven-transmembrane receptors. *Nat. Rev. Mol. Cell Biol.* 3:639–650.
7. Hopkins, A. L., and C. R. Groom. 2002. The druggable genome. *Nat. Rev. Drug Discov.* 1:727–730.
8. Oldham, W. M., and H. E. Hamm. 2006. Structural basis of function in heterotrimeric G proteins. *Q. Rev. Biophys.* 39:117–166.
9. Pucadyil, T. J., S. Kalipatnapu, and A. Chattopadhyay. 2005. The serotonin$_{1A}$ receptor: a representative member of the serotonin receptor family. *Cell. Mol. Neurobiol.* 25:553–580.
10. Müller, C. P., R. J. Carey, J. P. Huston, and M. A. D. S. Silva. 2007. Serotonin and psychostimulant addiction: focus on 5-HT$_{1A}$-receptors. *Prog. Neurobiol.* 81:133–178.
11. Gingrich, J. A., and R. Hen. 2001. Dissecting the role of the serotonin system in neuropsychiatric disorders using knockout mice. *Psychopharmacology (Berl.).* 155:1–10.
12. Fricker, A. D., C. Rios, L. A. Devi, and I. Gomes. 2005. Serotonin receptor activation leads to neurite outgrowth and neuronal survival. *Brain Res. Mol. Brain Res.* 138:228–235.
13. Pucadyil, T., S. Kalipatnapu, K. Harikumar, N. Rangaraj, S. Karnik, and A. Chattopadhyay. 2004. G-protein-dependent cell surface dynamics of the human serotonin$_{1A}$ receptor tagged to yellow fluorescent protein. *Biochemistry.* 43:15852–15862.
14. Cuatrecasas, P. 1974. Membrane receptors. *Annu. Rev. Biochem.* 43: 169–214.
15. Kahn, C. R. 1976. Membrane receptors for hormones and neurotransmitters. *J. Cell Biol.* 70:261–286.
16. Peters, R. 1988. Lateral mobility of proteins and lipids in the red cell membrane and the activation of adenylate cyclase by β-adrenergic receptors. *FEBS Lett.* 234:1–7.
17. Tank, D. W., E. S. Wu, and W. W. Webb. 1982. Enhanced molecular diffusibility in muscle membrane blebs: release of lateral constraints. *J. Cell Biol.* 92:207–212.
18. Berk, D. A., and R. M. Hochmuth. 1992. Lateral mobility of integral proteins in red blood cell tethers. *Biophys. J.* 61:9–18.
19. Fujiwara, T., K. Ritchie, H. Murakoshi, K. Jacobson, and A. Kusumi. 2002. Phospholipids undergo hop diffusion in compartmentalized cell membrane. *J. Cell Biol.* 157:1071–1081.
20. Kusumi, A., H. Murakoshi, K. Murase, and T. Fujiwara. 2005. Single-molecule imaging of diffusion, recruitment, and activation of signaling molecules in living cells. *In* Biophysical Aspects of Transmembrane Signaling. S. Damjanovich, editor. Springer Series in Biophysics. Springer-Verlag, Berlin. 123–152.
21. Smith, P. K., R. I. Krohn, G. T. Hermanson, A. K. Mallia, F. H. Gartner, M. D. Provenzano, E. K. Fujimoto, N. M. Goeke, B. J. Olson, and D. C. Klenk. 1985. Measurement of protein using bicinchoninic acid. *Anal. Biochem.* 150:76–85.
22. Nordstedt, C., and B. B. Fredholm. 1990. A modification of a protein-binding method for rapid quantification of cAMP in cell-culture supernatants and body fluid. *Anal. Biochem.* 189:231–234.
23. Umenishi, F., J.-M. Verbavatz, and A. S. Verkman. 2000. cAMP regulated membrane diffusion of a green fluorescent protein-aquaporin 2 chimera. *Biophys. J.* 78:1024–1035.
24. Pucadyil, T. J., and A. Chattopadhyay. 2007. Cholesterol depletion induces dynamic confinement of the G-protein coupled serotonin$_{1A}$ receptor in the plasma membrane of living cells. *Biochim. Biophys. Acta.* 1768:655–668.
25. Crank, J. 1956. The Mathematics of Diffusion. Oxford University Press, London.
26. Soumpasis, D. M. 1983. Theoretical analysis of fluorescence photobleaching recovery experiments. *Biophys. J.* 41:95–97.
27. Sampath, P., and T. D. Pollard. 1991. Effects of cytochalasin, phalloidin, and pH on the elongation of actin filaments. *Biochemistry.* 30:1973–1980.
28. Schliwa, M. 1982. Action of cytochalasin D on cytoskeletal networks. *J. Cell Biol.* 92:79–91.

29. Nicolau, D. V., K. Burrage, R. G. Parton, and J. F. Hancock. 2006. Identifying optimal lipid raft characteristics required to promote nanoscale protein-protein interactions on the plasma membrane. *Mol. Cell. Biol.* 26:313–323.
30. Lamb, N. J., A. Fernandez, M. A. Conti, R. Adelstein, D. B. Glass, W. J. Welch, and J. R. Feramisco. 1988. Regulation of actin microfilament integrity in living nonmuscle cells by the cAMP-dependent protein kinase and the myosin light chain kinase. *J. Cell Biol.* 106:1955–1971.
31. Dong, J. M., T. Leung, E. Manser, and L. Lim. 1998. cAMP-induced morphological changes are counteracted by the activated RhoA small GTPase and the Rho kinase ROKα. *J. Biol. Chem.* 273:22554–22562.
32. Howe, A. K. 2004. Regulation of actin-based cell migration by cAMP/PKA. *Biochim. Biophys. Acta.* 1692:159–174.
33. Szászi, K., K. Kurashima, K. Kaibuchi, S. Grinstein, and J. Orlowski. 2001. Role of the cytoskeleton in mediating cAMP-dependent protein kinase inhibition of the epithelial Na+/H+ exchanger NHE3. *J. Biol. Chem.* 276:40761–40768.
34. Fischer, H., B. Illek, and T. E. Machen. 1995. The actin filament disrupter cytochalasin D activates the recombinant cystic fibrosis transmembrane conductance regulator Cl-channel in mouse 3T3 fibroblasts. *J. Physiol.* 489:745–754.
35. Harikumar, K. G., and A. Chattopadhyay. 1999. Differential discrimination of G-protein coupling of serotonin$_{1A}$ receptors from bovine hippocampus by an agonist and an antagonist. *FEBS Lett.* 457:389–392.
36. Zimmerberg, J. 2006. Membrane biophysics. *Curr. Biol.* 16:R272–R276.
37. Saffman, P. G., and M. Delbrück. 1975. Brownian motion in biological membranes. *Proc. Natl. Acad. Sci. USA.* 72:3111–3113.
38. Gambin, Y., R. Lopez-Esparza, M. Reffay, E. Sierecki, N. S. Gov, M. Genest, R. S. Hodges, and W. Urbach. 2006. Lateral mobility of proteins in liquid membranes revisited. *Proc. Natl. Acad. Sci. USA.* 103:2098–2102.
39. Suzuki, K., K. Ritchie, E. Kajikawa, T. Fujiwara, and A. Kusumi. 2005. Rapid hop diffusion of a G-protein-coupled receptor in the plasma membrane as revealed by single-molecule techniques. *Biophys. J.* 88:3659–3680.
40. Saxton, M. J. 2001. Anomalous subdiffusion in fluorescence photobleaching recovery: a Monte Carlo study. *Biophys. J.* 81:2226–2240.
41. Horvat, R. D., S. Nelson, C. M. Clay, B. G. Barisas, and D. A. Roess. 1999. Intrinsically fluorescent luteinizing hormone receptor demonstrates hormone-driven aggregation. *Biochem. Biophys. Res. Commun.* 255:382–385.
42. Nelson, S., R. D. Horvat, J. Malvey, D. A. Roess, B. G. Barisas, and C. M. Clay. 1999. Characterization of an intrinsically fluorescent gonadotropin-releasing hormone receptor and effects of ligand binding on receptor lateral diffusion. *Endocrinology.* 140:950–957.
43. Kwik, J., S. Boyle, D. Fooksman, L. Margolis, M. P. Sheetz, and M. Edidin. 2003. Membrane cholesterol, lateral mobility, and the phosphatidylinositol 4,5-bisphosphate-dependent organization of cell actin. *Proc. Natl. Acad. Sci. USA.* 100:13964–13969.
44. Liu, A. P., and D. A. Fletcher. 2006. Actin polymerization serves as a membrane domain switch in model lipid bilayers. *Biophys. J.* 91:4064–4070.
45. Sun, M., N. Northup, F. Marga, T. Huber, F. J. Byfield, I. Levitan, and G. Forgacs. 2007. The effect of cellular cholesterol on membrane-cytoskeleton adhesion. *J. Cell Sci.* 120:2223–2231.
46. Gether, U. 2000. Uncovering molecular mechanisms involved in activation of G protein-coupled receptors. *Endocr. Rev.* 21:90–113.
47. Hamm, H. E. 2001. How activated receptors couple to G proteins. *Proc. Natl. Acad. Sci. USA.* 98:4819–4821.
48. Calvert, P. D., V. I. Govardovskii, N. Krasnoperova, R. E. Anderson, J. Lem, and C. L. Makino. 2001. Membrane protein diffusion sets the speed of rod phototransduction. *Nature.* 411:90–94.
49. Neubig, R. R. 1994. Membrane organization in G-protein mechanisms. *FASEB J.* 8:939–946.
50. Huang, C., J. R. Hepler, L. T. Chen, A. G. Gilman, R. G. Anderson, and S. M. Mumby. 1997. Organization of G proteins and adenylyl cyclase at the plasma membrane. *Mol. Biol. Cell.* 8:2365–2378.
51. Hein, P., M. Frank, C. Hoffmann, M. J. Lohse, and M. Bünemann. 2005. Dynamics of receptor/G protein coupling in living cells. *EMBO J.* 24:4106–4114.
52. Kwon, G., D. Axelrod, and R. R. Neubig. 1994. Lateral mobility of tetramethylrhodamine (TMR) labelled G protein α and $\beta\gamma$ subunits in NG 108–15 cells. *Cell. Signal.* 6:663–679.
53. Rebois, R. V., M. Robitaille, C. Galés, D. J. Dupré, A. Baragli, P. Trieu, N. Ethier, M. Bouvier, and T. E. Hébert. 2006. Heterotrimeric G proteins form stable complexes with adenylyl cyclase and Kir3.1 channels in living cells. *J. Cell Sci.* 119:2807–2818.
54. Hur, E.-M., and K.-T. Kim. 2002. G protein-coupled receptor signalling and cross-talk: achieving rapidity and specificity. *Cell. Signal.* 14:397–405.
55. Head, B. P., H. H. Patel, D. M. Roth, F. Murray, J. S. Swaney, I. R. Niesman, M. G. Farquhar, and P. A. Insel. 2006. Microtubules and actin microfilaments regulate lipid raft/caveolae localization of adenylyl cyclase signaling components. *J. Biol. Chem.* 281:26391–26399.
56. Jans, D. A., R. Peters, P. Jans, and F. Fahrenholz. 1991. Vasopressin V_2 receptor mobile fraction and ligand-dependent adenylate cyclase activity are directly correlated in LLC-PK1 renal epithelial cells. *J. Cell Biol.* 114:53–60.
57. Bünemann, M., M. Frank, and M. J. Lohse. 2003. Gi protein activation in intact cells involves subunit rearrangement rather than dissociation. *Proc. Natl. Acad. Sci. USA.* 100:16077–16082.
58. Mellgren, R. L. 2008. Detergent-resistant membrane subfractions containing proteins of plasma membrane, mitochondrial, and internal membrane origins. *J. Biochem. Biophys. Methods.* 70:1029–1036.
59. Haggie, P. M., B. A. Stanton, and A. S. Verkman. 2004. Increased diffusional mobility of CFTR at the plasma membrane after deletion of its C-terminal PDZ binding motif. *J. Biol. Chem.* 279:5494–5500.
60. Xiao, H., V. M. Hapiak, K. A. Smith, L. Lin, R. J. Hobson, J. Plenefisch, and R. Komuniecki. 2006. SER-1, a *Caenorhabditis elegans* 5-HT$_2$-like receptor, and a multi-PDZ domain containing protein (MPZ-1) interact in vulval muscle to facilitate serotonin-stimulated egg-laying. *Dev. Biol.* 298:379–391.
61. Turner, J. H., A. K. Gelasco, and J. R. Raymond. 2004. Calmodulin interacts with the third intracellular loop of the serotonin 5-hydroxytryptamine$_{1A}$ receptor at two distinct sites: putative role in receptor phosphorylation by protein kinase C. *J. Biol. Chem.* 279:17027–17037.
62. Kulkarni, R. P., M. Bak-Maier, and S. E. Fraser. 2007. Differences in protein mobility between pioneer versus follower growth cones. *Proc. Natl. Acad. Sci. USA.* 104:1207–1212.
63. Zaccolo, M., G. D. Benedetto, V. Lissandron, L. Mancuso, A. Terrin, and I. Zamparo. 2006. Restricted diffusion of a freely diffusible second messenger: mechanisms underlying compartmentalized cAMP signalling. *Biochem. Soc. Trans.* 34:495–497.
64. Song, H. J., G. L. Ming, and M. M. Poo. 1997. cAMP-induced switching in turning direction of nerve growth cones. *Nature.* 388:275–279.
65. Ming, G. L., H. J. Song, B. Berninger, C. E. Holt, M. Tessier-Lavigne, and M. M. Poo. 1997. cAMP-dependent growth cone guidance by netrin-1. *Neuron.* 19:1225–1235.